Element specific spin and orbital moments of nanoscale CoFeB amorphous thin films on GaAs(100)

Yu Yan, Cong Lu, Hongqing Tu, Xianyang Lu, Wenqing Liu, Junlin Wang, Lei Ye, Iain Will, Balati Kuerbanjiang, Vlado K. Lazarov, Jing Wu, Johnny Wong, Biao You, Jun Du, Rong Zhang, and Yongbing Xu

Citation: AIP Advances **6**, 095011 (2016); doi: 10.1063/1.4962994
View online: http://dx.doi.org/10.1063/1.4962994
View Table of Contents: http://scitation.aip.org/content/aip/journal/adva/6/9?ver=pdfcov
Published by the AIP Publishing

Articles you may be interested in

Nonreciprocal behavior of the spin pumping in ultra-thin film of CoFeB
J. Appl. Phys. **119**, 133903 (2016); 10.1063/1.4945028

Spin and orbital moments of nanoscale Fe3O4 epitaxial thin film on MgO/GaAs(100)
Appl. Phys. Lett. **104**, 142407 (2014); 10.1063/1.4871001

Magnetostriction effect of amorphous CoFeB thin films and application in spin-dependent tunnel junctions
J. Appl. Phys. **97**, 10C906 (2005); 10.1063/1.1848355

Annealing behavior of amorphous ferromagnetic Co-Fe-B and Fe-B thin films
J. Appl. Phys. **52**, 2928 (1981); 10.1063/1.329029

Abstract: Annealing behavior of amorphous ferromagnetic Co-Fe-B and Fe-B thin films
J. Appl. Phys. **50**, 1604 (1979); 10.1063/1.327263

Reuse of AIP Publishing content is subject to the terms at: https://publishing.aip.org/authors/rights-and-permissions. Download to IP: 134.219.64.12 On: Tue, 29 Nov 2016 11:20:30

Element specific spin and orbital moments of nanoscale CoFeB amorphous thin films on GaAs(100)

Yu Yan,[1,2] Cong Lu,[2] Hongqing Tu,[3] Xianyang Lu,[4] Wenqing Liu,[1,2] Junlin Wang,[2] Lei Ye,[5] Iain Will,[2] Balati Kuerbanjiang,[4] Vlado K. Lazarov,[4] Jing Wu,[1,4] Johnny Wong,[1] Biao You,[3] Jun Du,[3,a] Rong Zhang[1] and Yongbing Xu[1,2,b]

[1]*York-Nanjing International Center of Spintronics (YNICS), Jiangsu Provincial Key Laboratory of Advanced Photonic and Electronic Material, Jiangsu Procincial Key Laboratory for Nanotechnology, School of Electronic Science and Engineering, Nanjing University, Nanjing 210093, China*

[2]*Spintronics and Nanodevice laboratory, Department of Electronics, University of York, YO10 5DD, United Kingdom*

[3]*National Laboratory of Solid State Microstructures and Department of Physics, Nanjing University, Nanjing 210093, China*

[4]*Department of Physics, University of York, YO10 5DD, United Kingdom*

[5]*College of Communication Engineering, Chongqing University, Chongqing 400044, China*

(Received 14 June 2016; accepted 6 September 2016; published online 13 September 2016)

CoFeB amorphous films have been synthesized on GaAs(100) and studied with X-ray magnetic circular dichroism (XMCD) and transmission electron microscopy (TEM). We have found that the ratios of the orbital to spin magnetic moments of both the Co and Fe in the ultrathin amorphous film have been enhanced by more than 300% compared with those of the bulk crystalline Co and Fe, and specifically a large orbital moment of 0.56 μ_B from the Co atoms has been observed and at the same time the spin moment of the Co atoms remains comparable to that of the bulk hcp Co. The results indicate that the large uniaxial magnetic anisotropy (UMA) observed in the ultrathin CoFeB film on GaAs(100) is related to the enhanced spin-orbital coupling of the Co atoms in the CoFeB. This work offers experimental evidences of the correlation between the UMA and the element specific spin and orbital moments in the CoFeB amorphous film on the GaAs(100) substrate, which is of significance for spintronics applications. © *2016 Author(s). All article content, except where otherwise noted, is licensed under a Creative Commons Attribution (CC BY) license (http://creativecommons.org/licenses/by/4.0/).* [http://dx.doi.org/10.1063/1.4962994]

The magnetic CoFeB amorphous alloys have attracted renewed interests for the applications in the next generation spintronics devices such as magnetic random access memory (MRAM)[1–3] and spin field effect transistor (SpinFET).[4,5] For the development of SpinFET, the structure and magnetic properties of various ferromagnetic (FM) thin films on top of semiconductors (SC) such as GaAs and Si have been extensively studied over the last two decades.[6–10] One of the most interesting discoveries is a uniaxial magnetic anisotropy (UMA) observed in several FM/SC,[11,12] when the thickness of the FM layer is reduced down to nanometer scale. For example, the bcc Fe films on GaAs(100) substrates display the UMA from 1.4 nm to 11.5 nm,[13] and for bcc CoFe on GaAs(100), the UMA has been found between 1.1 and 1.7 nm.[14] In the crystalline FM/SC systems, the magnetocrystalline anisotropy (MCA) might also change with the reduction of the film thickness.[15] Generally, the UMA and MCA have been found to co-exist in most of the common FM/SC film systems.[16] To exclude the contribution from MCA, and thus focus on the UMA in the FM/SC film system, an effective method would to be to alloy the ferromagnetic film with metalloid material in order to create an amorphous magnetic thin films. Approximately 20% Boron alloyed with CoFe compound has been proven desirable.

[a]Electronic mail: jdu@nju.edu.cn
[b]Electronic mail: yongbing.xu@york.ac.uk

 © Author(s) 2016

Reuse of AIP Publishing content is subject to the terms at: https://publishing.aip.org/authors/rights-and-permissions. Download to IP: 134.219.64.12 On: Tue, 29 Nov 2016 11:20:30

The additional Boron only slightly reduces the film Curie temperature and saturation field while completely destroy its crystallinity.[17] Recent research indeed found that the amorphous CoFeB films deposited on top of GaAs still exhibit the UMA.[18,19] Several models have been proposed including, bond-orientational anisotropy (BOA),[6,20] Neel-Taniguchi directional pair-ordering model and random anisotropy model,[21] in order to explain the origin of the UMA in CoFeB/GaAs. According to the BOA model, a medium-to-long range microstructural anisotropy is responsible for the UMA. The Neel-Taniguchi directional pair-ordering model introduces anisotropy via the dipole-like coupling between individual atom-pairs, leading to anisotropic chemical ordering of near-neighbour atoms in randomly oriented coordination. The random anisotropy model emphasizes the break of the rotational symmetry of the Hamiltonian, which gives rise to the hard magnetic behaviour even in random amorphous magnets. The origin of the UMA has also been suggested to be due to the enhanced spin-orbit coupling and interface interaction,[22] which is controlled by the orbital moment and the substrate crystal lattice.[23] The orbital moment has been found to have a more important role than the spin moment in giving rise to the uniaxial magnetic anisotropy.[24,25] Hindmarch et al[22] compared the UMA of CoFeB on different substrates of AlGaAs/GaAs and AlGaAs. As shown in Table I, they found a much stronger UMA (50 Oe) on AlGaAs/GaAs substrate associated with an enhancement of the orbital to spin magnetic moments ratios m_{ratio} of both the Fe and Co sites, and the uniaxial magnetic anisotropy field H_k of the UMA was found to be proportional to the m_{ratio}. Very recently, we have found a larger H_k up to 270 Oe in a CoFeB/GaAs(100) system, which is much stronger than any previously reported values.[26] In this letter, we report a study of the spin and orbital moments in this CoFeB/GaAs(100) system using XMCD along with TEM and VSM. The large UMA observed in the CoFeB/GaAs(100) calls for a closer study of the spin and orbital moments and the spin-orbital coupling, which may play an important role in this system. It is well known that orbital angular moment plays a dominant role in determining the strength of magnetocrystalline and uniaxial magnetic anisotropy[25] and XMCD technique is capable of probing directly the element specific orbital and spin moments.[24,27–29]

The $Co_{56}Fe_{24}B_{20}$ films were grown on GaAs(100) substrates. Before deposition of the CoFeB film, the substrate surface was etched and cleaned. First the contaminants of substrate surface were removed using acetone, ethanol and deionized water. The second step was to remove the oxide layer by immersion of the substrate into an HCl/H2O (1:1) solution for 50 s. The third step is to create a flat surface for film deposition, which is acheved by inducing substrate surface reconstruction. The cleaned substrate was loaded into an ultrahigh-vacuum chamber with a base pressure lower than 8×10^{-9} mbar and heated to 450 °C for 15 min and a further 30 min at 580 °C (annealing pressure lower than 8×10^{-8} mbar) to obtain a clean and smooth surface.[19] The surface is allowed to cool to room temperature prior to film growth. The CoFeB films were prepared by DC magnetron sputtering deposition in 0.3 Pa argon (99.99%) at room temperature with a base pressure lower than 8×10^{-6} Pa. A target containing $Co_{56}Fe_{24}B_{20}$ was used to deposit the magnetic CoFeB layer, with a thickness of 3.5 nm. Finally a 2 nm Ta film was deposited as a capping layer to prevent the CoFeB film from oxidization.

TABLE I. Orbital moments, spin moments and orbit to spin ratio of the Fe and Co from various CoFeB samples in units of μ_B/atom.

Sample	UMA(Oe)	Element	$m_{orb}(\mu_B)$	$m_{spin}(\mu_B)$	m_{ratio}
Ta/$Co_{56}Fe_{24}B_{20}$(3.5nm)/GaAs(100)	270	Fe	0.30 ± 0.03	1.17 ± 0.03	0.26
		Co	0.56 ± 0.03	1.53 ± 0.03	0.36
Ta/$Co_{40}Fe_{40}B_{20}$(3.5nm)/GaAs(100)/AlGaAs(100)[17]	50	Fe			0.45
		Co			0.38
Ta/$Co_{40}Fe_{40}B_{20}$(3.5nm)/AlGaAs(100)[17]	25	Fe			0.34
		Co			0.19
Ta/$Co_{40}Fe_{40}B_{20}$(2.0nm)/MgO[36]		Fe	0.27 ± 0.03	1.77 ± 0.03	0.15
		Co	0.17 ± 0.03	0.90 ± 0.03	0.19
Bulk bcc Fe[31,33]		Fe	0.09 ± 0.05	1.98 ± 0.05	0.04
Bulk hcp Co[31,33]		Co	0.15 ± 0.05	1.55 ± 0.05	0.10

Reuse of AIP Publishing content is subject to the terms at: https://publishing.aip.org/authors/rights-and-permissions. Download to IP: 134.219.64.12 On: Tue, 29 Nov 2016 11:20:30

Structural properties of the grown films were studied by JEOL 2200FS double aberration corrected (scanning) transmission electron microscope (S) TEM. Cross-sectional TEM specimens were prepared using conventional methods that include mechanical thinning and polishing followed by Ar ion milling in order to achieve electron transparency.[30]

The in-plane magnetic hysteresis (*M-H*) loops were measured using a Vector Magnetometer Model 10 VSM and Vector measurement system. As a strong uniaxial anisotropy field (H_k) as large as 270 Oe was expected,[26] the VSM measurement was conducted using a maximum magnetic field of 400 Oe to ensure the samples were fully saturated. The samples were measured at angles 0° and 90°, *i.e.* along the hard and easy axis, respectively.

XMCD measurements were performed at normal incidence to the Ta/CoFeB/GaAs(100) sample in the MAX Lab I1011 station. The XMCD spectra were measured at both positive and negative applied fields.[31] The data was collected by Total Electron Yield (TEY) detector in the analysis chamber under a magnetic field of 2000 Oe. This was the operational limit of the magnet in the station, as the magnetic field has to be set at a relatively low value in order to limit magnet overheating.[32] The magnetization hysteresis loop of the CoFeB film along the out-of-plane direction was measured by a Polar MOKE, and the saturation field was found be to as large as 12000 Oe. It is apparent, from Fig.1(b), that for the out-of-plane direction, the magnetic field used during the XMCD measurements was not sufficient to saturate the sample. It is for this reason that, the spin and orbital moments obtained from the XMCD were scaled up to get the saturation value. During this work, all the measurements were performed at room temperature.

Fig.1(a) shows the in-plane magnetic hysteresis (M-H) loop measured by VSM along the EA and HA for the CoFeB/GaAs(100) sample. The figure shows a clear UMA with a well-defined EA and HA axis. The value of the UMA field (H_k) can be obtained from the saturation field along the HA direction. Furthermore, the effective uniaxial anisotropy constant K_u^{eff} can be calculated by[6]

$$K_u^{eff} = (H_k \cdot M_S)/2 \tag{1}$$

where the M_s is saturation magnetization and H_k is the saturation field along the HA.

It can be seen from the Fig.1 (a) that H_k has a value of 270 Oe, confirming our previous observation of a large UMA in the CoFeB/GaAs(100) system. According to the saturation moment and thickness measurement, the value of M_s is estimated to be 977 Gs. The value of K_u^{eff} is thus determined to be 13 kJ/m^3, which is much larger than the reported values of K_u^{eff}=2 kJ/m^3 and 8 kJ/m^3 by[17,33] respectively. We would also like to note that the K_u^{eff} value of the CoFeB films on GaAs(100) has the largest value when compared to films grown on GaAs(110) and GaAs(111) substrate orientations, e.g. value of 1 kJ/m^3 and 0.6 kJ/m^3 on GaAs(110) and GaAs(111) substrates respectively.[10,22,34]

The hysteresis loop for the CoFeB/GaAs(100) sample along the perpendicular (out of plane) direction measured by a Polar MOKE stated (Fig.1(b)), shows that along this direction is the hard magnetization axis. As state earlier, when making the XMCD measurement along perpendicular

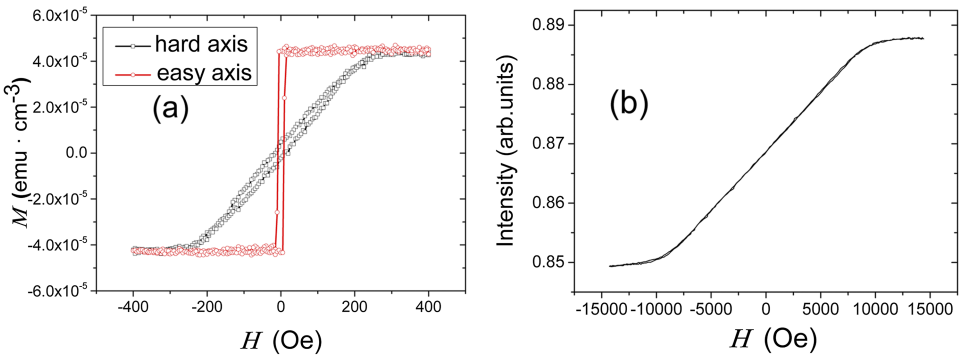

FIG. 1. (a) In-plane M-H loops along both the EA (easy axis) and HA (hard axis) for the CoFeB film deposited on GaAs(100) substrates by VSM measurement. M and H represent the magnetic moment and applied magnetic field, respectively. Figure (b) shows the Polar MOKE loop for the out-of-plane direction of the CoFeB film.

Reuse of AIP Publishing content is subject to the terms at: https://publishing.aip.org/authors/rights-and-permissions. Download to IP: 134.219.64.12 On: Tue, 29 Nov 2016 11:20:30

direction, the applied magnetic field of 2000 Oe was not large enough to saturate the sample. From the perpendicular loop in figure 1(b), the saturation magnetic field is determined to be 10189 Oe. Hence the data of spin and orbital moments from the XMCD have been scaled up by a factor of 5.09 as based on comparison of the magnetization at 2000 Oe and that at saturation, included in Table I.

High resolution cross-sectional TEM image of the structure is shown in Fig.2. The films thicknesses of 3.5 nm and 2 nm for CoFeB and Ta, respectively, match the growth settings. The missing lattice fringes and no distinctive rings or diffraction spots in the digital diffractogram from film area show that the CoFeB film structure is amorphous. We also note, similarly to[35], that formation of CoFeB crystalline monolayers at the very interface cannot be ruled out. Due to mass contrast a clear distinction between the Ta and CoFeB can be observed as well as between the CoFeB and GaAs due to the single crystal structure of the GaAs substrate and the amorphous structure of the CoFeB.

X-ray absorption spectra (XAS) of the Co and Fe L_2 and L_3 edges for CoFeB on GaAs(100) are shown in Fig. 3 (a) and (c) respectively, in which u_+ and u_- are the absorption coefficients under antiparallel and parallel magnetic fields to the photon incident direction. Figure 3 shows the XMCD spectra for the Fe and Co L-edges of the CoFeB film. According to XMCD sum rules, the orbital (m_{orb}) and spin (m_{spin}) magnetic moments and the ratio (m_{ratio}) of m_{orb} to m_{spin} can be determined from XAS and XMCD spectra by the following equations:[31]

$$m_{orb} = -\frac{4\int_{L3+L2}(u_+ - u_-)d\omega}{3\int_{L3+L2}(u_+ + u_-)d\omega}(10 - n_{3d})\left(1 + \frac{7\langle T_Z\rangle}{2}\langle S_Z\rangle\right) \tag{2}$$

$$m_{spin} = -\frac{6\int_{L3}(u_+ - u_-)d\omega - 4\int_{L3+L2}(u_+ - u_-)d\omega}{\int_{L3+L2}(u_+ + u_-)d\omega}\left(1 + \frac{7\langle T_Z\rangle}{2}\langle S_Z\rangle\right) \tag{3}$$

$$m_{ratio} = \frac{m_{orb}}{m_{spin}} \tag{4}$$

Where m_{orb} and m_{spin} are the orbital and spin magnetic moments in units u_B/atom, respectively, and n_{3d} is the 3d electron occupation number of the specific transition metal atom. L_3 and L_2 denote the integration ranges. $\langle T_Z\rangle$ is the expectation value of magnetic dipole and S_Z is equal to half of m_{spin} in Hartree atomic units.[22] The spin and orbital moments are also dependent on the d-band hole density in CoFeB and the intensity of the polarized x-ray in XMCD measurement. We would like to note that it is a controversial issue about the 3d hole numbers of Fe and Co in magnetic amorphous films. While Cui et al[36] use the m_{orb}/n_h to present their data, Kanai et al[37] have calculated the hole

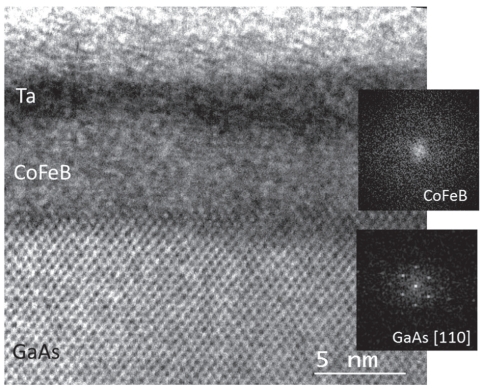

FIG. 2. Cross-sectional bright-field scanning TEM micrograph of CoFeB/GaAs(100) in [110] view. The amorphous nature of the CoFeB is clearly shown by the inset digital diffractogram calculated from film area in contrast to single crystal structure of the GaAs shown by atomic planes cross fringes and Bragg reflections in the digital diffractogram (inset).

Reuse of AIP Publishing content is subject to the terms at: https://publishing.aip.org/authors/rights-and-permissions. Download to IP: 134.219.64.12 On: Tue, 29 Nov 2016 11:20:30

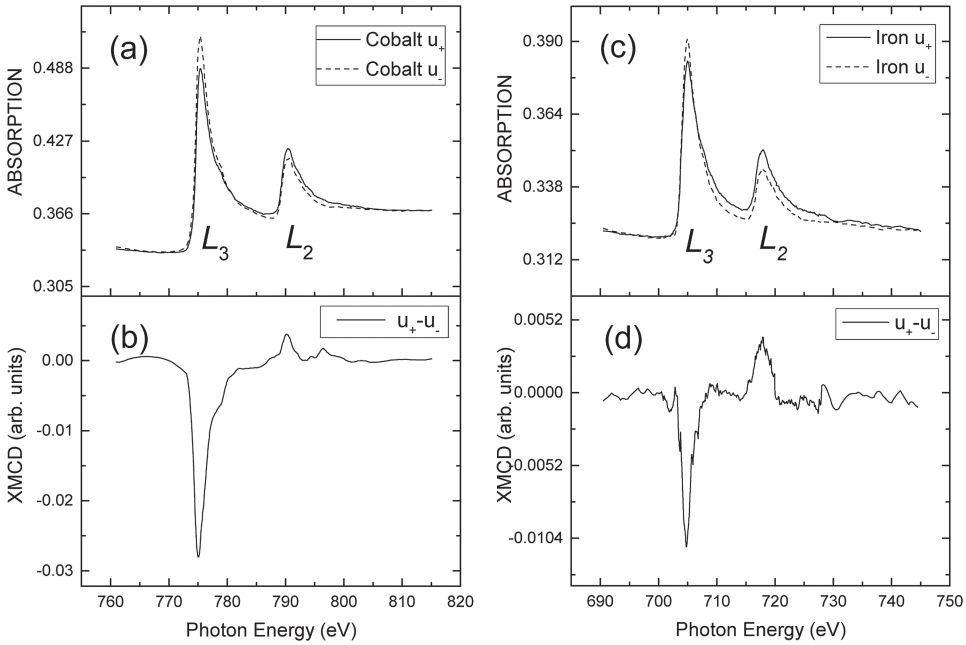

FIG. 3. XAS and XMCD spectra of the Co and Fe atoms at the L_2 and L_3 edges in the CoFeB/GaAs(100): (a) and (c) are the XAS absorption spectra and (b) and (d) are the XMCD for Co and Fe, respectively.

numbers of Co and Fe in the amorphous films by first-principles calculations, and they found the similar values to those of the bulk Fe and Co films.[34,37] In this work, we have used the values of n_{3d} for Fe and Co of 6.61 and 7.51, respectively, from[37] to calculate the spin and orbital moment of Co and Fe in the CoFeB film.

The values of m_{orb}, m_{spin} and m_{ratio} are all determined from XMCD data, and the results are listed in Table I along with those reported in the literatures. Firstly, from comparing the amorphous films and the crystalline elements, one result is confirmed: the orbital moments of the Fe and Co in the amorphous films are larger than that of the crystalline bcc Fe and hcp Co. While the spin moment of the Fe atoms in the CoFeB is much reduced compared with to that of bcc Fe, the spin moment of the Co atoms remains as large as 1.53 μ_B, which is almost the same as that of the hcp Co. As shown in Table I, the orbital to spin ratios m_{ratio} of the Co and Fe in the amorphous CoFeB film have been enhanced by 300% compared to those of the hcp Co and the bcc Fe.

Pervious work indicated that the stronger UMA for CoFeB on GaAs(100)/AlGaAs(100) is due to the enhancement of m_{ratio} as they found that m_{ratio} has been increased from 0.19 to 0.38 for Co and 0.34 to 0.45 for Fe when the UMA is increased from 25 Oe to 50 Oe.[17,26,37] Though the UMA in our sample was found to be as large as 270 Oe, the values of m_{ratio} show a comparable enhancement of 0.36 for Co and 0.26 for Fe. This shows that the UMA is associated with the enhancement of the orbital moments but does not vary linearly with the m_{ratio}.

One of the most striking results from the measurement (as shown in Table I) are that the spin and orbital moments of the Co atoms are significantly larger than those of the Fe atoms. When considering the value of the m_{ratio}, we can see that the Co atoms also have a larger value than that of the Fe atoms. The orbital moment of the Co atom in the CoFeB have been enhanced by more than 370% in comparison to the orbital moment of the crystalline hcp Co. This suggests that in the CoFeB(100) amorphous film, the Co atoms at the interface with the GaAs contribute more than Fe to the UMA. Our results indicate that the large UMA observed in the CoFeB(100)/GaAs(100) system comes from the large spin-orbit coupling of the Co atoms.

Spin-orbital coupling is a desired property in terms of the controllability by electric field in spintronic operation. The orbital moment of the Co atoms in the CoFeB/GaAs(100) has been found to be as large as 0.56 μ_B, which is the largest orbital moments reported in any amorphous magnetic alloys to the best of our knowledge.

Reuse of AIP Publishing content is subject to the terms at: https://publishing.aip.org/authors/rights-and-permissions. Download to IP: 134.219.64.12 On: Tue, 29 Nov 2016 11:20:30

In conclusion, we have investigated uniaxial magnetic anisotropy and the element specific spin and orbital moments in the CoFeB(100)/GaAs system by magnetization measurement, XMCD measurement and sum rule calculations. The results obtained by VSM measurements confirmed that the UMA can achieve as large as 270 Oe, which is among the largest of the UMA observed in any CoFeB amorphous alloys. XMCD measurements reveal that the UMA is correlated with a strong spin-orbit coupling related to the enhanced orbital to spin moment ratios of both Fe and Co in the CoFeB. More importantly, the spin moment of the Co has been found to remain as large as that of the crystalline hcp Co, and the orbital moments is enhanced by more than 370%, suggesting the dominate contribution of the spin-orbit coupling of the Co atoms to the UMA in the CoFeB(100)/GaAs amorphous film. These results would be useful for understanding the fundamental magnetic properties of the amorphous CoFeB films, which could be important for the applications of this class of materials in the next generation spintronics devices including the MRAM and SpinFET, where the functions of data process and storage could be integrated in a single device.

This work is supported by the National Natural Science Foundations of China (Grants No. 61274102, 11304148, 21173040), Natural Science Foundations of Jiangsu Province (Grants No. BK20130016 and BK20122322) and EPSRC UK (EP/K03278X/I), EPSRC, (EP/G010064/1).

[1] J. H. Kim, J. B. Lee, G. G. An, S. M. Yang, W. S. Chung, H. S. Park, and J. P. Hong, Sci. Rep. **5** (2015).
[2] S. Ikeda, K. Miura, H. Yamamoto, K. Mizunuma, H. D. Gan, M. Endo, S. Kanai, J. Hayakawa, F. Matsukura, and H. Ohno, Nat. Mater. **9**, 721 (2010).
[3] J. M. Teixeira, R. F. A. Silva, J. Ventura, A. M. Pereira, F. Carpinteiro, J. P. Araujo, J. B. Sousa, S. Cardoso, R. Ferreira, and P. P. Freitas, Mat. Sci. Eng.: B **126**, 180 (2006).
[4] S. Sugahara and M. Tanaka, Appl. Phys. Lett. **84**, 2307 (2004).
[5] C. Chappert, A. Fert, and F. N. Van Dau, Nat. Mater. **6**, 813 (2007).
[6] G. Wastlbauer and J. A. C. Bland, Adv. Phy. **54**, 137 (2005).
[7] Y. B. Xu, E. T. M. Kernohan, D. J. Freeland, A. J. A. C. Ercole, M. Tselepi, and J. A. C. Bland, Phys. Rev. B **58**, 890 (1998).
[8] J. Sinha, M. Hayashi, A. J. Kellock, S. Fukami, M. Yamanouchi, H. Sato, S. Ikeda, S. Mitani, S.-h. Yang, S. S. P. Parkin *et al.*, Appl. Phys. Lett. **102**, 242405 (2013).
[9] W. C. Tsai, S. C. Liao, H. C. Hou, C. T. Yen, Y. H. Wang, H. M. Tsai, F. H. Chang, H. J. Lin, and C.-H. Lai, Appl. Phys. Lett. **100**, 172414 (2012).
[10] F. Bianco, P. Bouchon, M. Sousa, G. Salis, and S. F. Alvarado, J. Appl. Phys. **104**, 83901 (2008).
[11] Y. B. Xu, E. T. M. Kernohan, M. Tselepi, J. A. C. Bland, and S. Holmes, Appl. Phys. Lett. **73**, 399 (1998).
[12] Y. B. Xu, S. Hassan, P. K. J. Wong, J. Wu, J. S. Claydon, Y. X. Lu, C. D. Damsgaard, J. B. Hansen, C. S. Jacobsen, Y. Zhai *et al.*, IEEE Trans. Magn. **44**, 2959 (2008).
[13] A. Ionescu, M. Tselepi, D. M. Gillingham, G. Wastlbauer, S. Steinmüller, H. E. Beere, D. A. Ritchie, and J. A. C. Bland, Phys. Rev. B **72**, 125404 (2005).
[14] M. Dumm, M. Zölfl, R. Moosbühler, M. Brockmann, T. Schmidt, and G. Bayreuther, J. Appl. Phys. **87**, 5457 (2000).
[15] P. Bruno, Phys. Rev. B **39**, 865 (1989).
[16] Y. B. Xu, D. J. Freeland, M. Tselepi, and J. A. C. Bland, Phys. Rev. B **62**, 1167 (2000).
[17] A. T. Hindmarch, A. W. Rushforth, R. P. Campion, C. H. Marrows, and B. L. Gallagher, Phys. Rev. B **83**, 212404 (2011).
[18] J. Hafner, M. Tegze, and C. Becker, Phys. Rev. B **49**, 285 (1994).
[19] D. M. Gillingham, M. Tselepi, A. Ionescu, S. J. Steinmuller, H. E. Beere, D. Ritchie, and J. A. C. Bland, Phys. Rev. B **76**, 214412 (2007).
[20] T. Egami, C. D. Graham, Jr., W. Dmowski, P. Zhou, and P. J. Glanders, IEEE Trans. Magn. **23**, 2269 (1987).
[21] R. Alben, J. J. Becker, and M. C. Chi, J. Appl. Phys. **49**, 1653 (1978).
[22] A. T. Hindmarch, C. J. Kinane, M. MacKenzie, J. N. Chapman, M. Henini, D. Taylor, D. A. Arena, J. Dvorak, B. J. Hickey, and C. Marrows, Phys. Rev. Lett. **100**, 117201 (2008).
[23] A. T. Hindmarch, D. A. Arena, K. J. Dempsey, M. Henini, and C. Marrows, Phys. Rev. B **81**, 100407 (2010).
[24] W. Q. Liu, Y. B. Xu, P. K. J. Wong, N. J. Maltby, S. P. Li, X. F. Wang, J. Du, B. You, J. Wu, P. Bencok, and R. Zhang, Appl. Phys. Lett. **104**, 142407 (2014).
[25] R. Skomski, A. Kashyap, and A. Enders, J. Appl. Phys. **109**, 07E143 (2011).
[26] H. Q. Tu, B. You, Y. Q. Zhang, Y. Gao, Y. B. Xu, and J. Du, IEEE Trans. Magn. **51**, 1 (2015).
[27] J. Trygg, B. Johansson, O. Eriksson, and J. M. Wills, Phys. Rev. Lett. **75**, 2871 (1995).
[28] Y. B. Xu, M. Tselepi, C. M. Guertler, C. A. F. Vaz, G. Wastlbauer, J. A. C. Bland, E. Dudzik, and G. van der Laan, J. Appl. Phys. **89**, 7156 (2001).
[29] W. Liu, L. He, Y. Zhou, K. Murata, M. C. Onbasli, C. A. Ross, Y. Jiang, Y. Wang, Y. Xu, R. Zhang, and K. L. Wang, AIP Adv **6**, 055813 (2016).
[30] L. Lari, S. Lea, C. Feeser, B. W. Wessels, and V. K. Lazarov, J. Appl. Phys. **111**, 07C311 (2012).
[31] C. T. Chen, Y. U. Idzerda, H. J. Lin, N. V. Smith, G. Meigs, E. Chaban, G. H. Ho, E. Pellegrin, and F. Sette, Phys. Rev. Lett. **75**, 152 (1995).
[32] I. A. Kowalik, G. Öhrwall, B. N. Jensen, R. Sankari, E. Wallén, U. Johansson, O. Karis, and D. Arvanitis, in J. Phys: Conf. Ser Vol. **211** (IOP Publishing, 2010) p. 012030.
[33] C. T. Chen, Y. U. Idzerda, H. J. Lin, G. Meigs, A. Chaiken, G. A. Prinz, and G. H. Ho, Phys. Rev. B **48**, 642 (1993).

Reuse of AIP Publishing content is subject to the terms at: https://publishing.aip.org/authors/rights-and-permissions. Download to IP: 134.219.64.12 On: Tue, 29 Nov 2016 11:20:30

[34] T. Ueno, J. Sinha, N. Inami, Y. Takeichi, S. Mitani, K. Ono, and M. Hayashi, Sci. Rep. **5** (2015).
[35] D. D. Djayaprawira, K. Tsunekawa, M. Nagai, H. Maehara, S. Yamagata, N. Watanabe, S. Yuasa, Y. Suzuki, and K. Ando, Appl. Phys. Lett. **86**, 092502 (2005).
[36] B. Cui, C. Song, Y. Y. Wang, W. S. Yan, F. Zeng, and F. Pan, J. Phys.:Condens. Matter **25**, 106003 (2013).
[37] S. Kanai, M. Tsujikawa, Y. Miura, M. Shirai, F. Matsukura, and H. Ohno, Appl. Phys. Lett. **105**, 222409 (2014).

Reuse of AIP Publishing content is subject to the terms at: https://publishing.aip.org/authors/rights-and-permissions. Download to IP: 134.219.64.12 On: Tue, 29 Nov 2016 11:20:30